City Research Online

City, University of London Institutional Repository

Experimental study on flexural behavior of new type of prestressed RPC sound barrier for high-speed rail

Running Head: Flexural behavior of new type of prestressed RPC sound barrier

Xia Cao[a], Zhen-Xuan Yang[a], Wan-Xu Zhu[a], Han-Ze Peng[b], Feng Fu[c] ORCID 0000-0002-9176-8159,
Long Wang[a]   and Kai Qian[a]

[a] Guangxi Key Laboratory of New Energy and Building Energy saving, Guilin University of Technology, Guilin 541004, China
[b] Tibet Zhongchi Group Co. LTD, Lhasa 850000, China
[c] School of Mathematics, Computer Science & Engineering, City, University of London, EC1V 0HB, U.K.

Correspondence

Wan-Xu Zhu,Guangxi Key Laboratory of New Energy and Building Energy saving, Guilin,

Email:zhuwanxu@vip.163.com,

Feng Fu，School of Mathematics, Computer Science & Engineering, City, University of London, EC1V 0HB, U.K.

cenffu@yahoo.co.uk

Abstract In this paper, 4-point bending tests of six prestressed Reactive Powder Concrete (RPC) sound barrier panel units were performed, the flexural behavior, deflection and failure modes of both in situ and prefabricated panels were studied. The results show that the major failure modes for in situ panels were bending failure. Prestressing the panels can effectively increase the cracking loads and improve stiffness of the in situ panels, but it cannot improve the ultimate flexural capacities. The ductility of the in situ panels decreased with the increase of prestressing degree. The stiffness of the prefabricated panels was improved by prestressing. Increasing the thickness of back and front plates, the ductility of the panels decreased accordingly, and the ductility of the prefabricated panels decreased more obviously than that of in situ panels. Based on the test results, considering tensile strength of RPC and prestressing stress, a modified formula

for flexural capacity of in situ panels was established. In the meantime, considering the "bridge" effect of steel fiber, the formulae to calculate the crack width and deflection at service limit state were also developed for future design.

Notation

B_s is the calculated short-term stiffness panel

c is the concrete cover thickness,

c_f is the coefficient of internal force of the member,

d_{eq} is the equivalent diameter of reinforcement in the tension zone,

E_c is the elastic modulus of concrete,

E_{el} is the elastic energy,

E_s is the elastic modulus of steel bar,

f is the calculated deflection of panel,

I_0 is the moment of inertia of conversion section,

k is the coefficient of the equivalent stress distribution map of the tension zone, reference [1], $k=\beta_t \lambda_f$,

l is the calculated span of panel,

l_c is the average spacing of cracks,

l_f/d_f is the ratio of length to diameter of steel fiber,

M is the bending moment of panel under the short-term combination of loads,

M_0 is the flexural capacity of prestressed panels

P is the load on panel,

U_{in} is the energy consumption,

W_0 is the elastic resistance moment of prestressed tension edge of conversion section of bending member,

W_{tot} is the sum of energy consumption and elastic energy,

x_t is the equivalent height of tension zone of the section，reference [2]，$x_t=h-x/\beta_1$，

α_1 and β_1 are the coefficients of the equivalent stress distribution map of the compression zone，for reactive powder concrete, reference [3], α_1 takes 0.85, β_1 takes 0.7,

α_{cr} is the coefficient of force characteristics of the member

β_B is the influence coefficient of steel fiber on short-term stiffness of bending member，β_B takes 0.354,

β_t is the influence coefficient of steel fiber on tensile strength of RPC, for bending member, β_t takes 1.3,

γ is the influence coefficient of section resistance moment，according to the Chinese concrete structure design specification, γ takes 1.35,

Δ_u is the ultimate deflection of unit panel,

Δ_y is the yield deflection of unit panel,

κ_{cr} is the ratio of cracking moment M_{cr} to maximum bending moment M_k,

λ is the prestressing degree,

λ_f is the characteristic parameter of steel fiber, $\lambda_f = \rho_f \cdot l_f / d_f$,

μ_{in} is the energy dissipation factor,

μ_Δ is the coefficient of deflection ductility,

ρ_f is the volume ratio of steel fiber，

ρ_{te} is the reinforcement ratio of tensile reinforcement,

σ'_{p0} is the stress of prestressed steel bar when concrete normal stress is equal to zero at all joints of longitudinal prestressing steel bar A'_p in the compression zone,

σ_{pc} is the pre-compression stress of concrete of tensile edge of prestressed flexural member,

σ_{sc} is the effective prestress to the edge tensile stress under the short-term effect of external load,

σ_{sk} is the equivalent stress of longitudinal tensile reinforcement when the loads are calculated by using a standard combination,

ψ is the uneven coefficient of strain of longitudinal steel in the crack of the concrete member,

1. Introduction

Due to the increasing speed of high-speed train, the sound barriers on both sides of the railway undergo higher than ever aerodynamic wind pressure when trains passing through. The ordinary concrete sound barriers are prone to crack or even break due to their low tensile strength. Therefore, their sound proof ability will be greatly deteriorated. Reactive Powder Concrete [4-7] (RPC) is a new environmentally friendly material with excellent properties such as high strength, high toughness and high durability. It can improve the crack resistance of the sound barrier by replacing ordinary concrete with reactive powder concrete. During the transportation and installation process, and under the effect of aerodynamic wind pressure of the train and wind load, the unit panel is prone to cracks due to the hollow structure of the RPC sound barrier unit panel and the relatively thin front and back panel. In order to control the occurrence and development of cracks, prestressing is applied by directly stretching the longitudinal reinforcement to improve the crack resistance of the unit panel. Homma et al [8] proposed an electromagnetically controlled swingable sound barrier to prevent excessive deformation. G. R. Watts et al [9] studied the effects of different cap shapes, wind speeds and wind directions on the noise reduction of sound barriers. Studies had shown that the T-shaped and multi-edge caps for sound-absorbing structures had the best noise reduction effect. Zhang et al [10] carried out fatigue tests on four prestressed concrete cantilever panels under repeated bending. The results show that fatigue performance under bending was better than that under axial loads. The effective prestress loss is between 3% and 6% due to fatigue loading. Lv et al [11] studied seismic behavior of uni-section and tapered section curved prestressed in situ concrete sound barriers. The results show that the hysteresis behavior is excellent. He et al [12] carried out the bending test of the GRC sound barrier panels and verified that the calculation theory of the flexural capacity of conventional concrete was suitable for GRC concrete sound barrier panels.

Although a large number of experimental and theoretical studies have been carried out on concrete sound barriers, little research has been done on the prestressed reactive powder concrete sound barrier. In this paper, the flexural capacity tests of the in situ and prefabricated RPC sound barrier with different prestressing degrees are carried out to analyze the flexural behavior of the prestressed RPC sound barrier unit panels.

2. Experimental program

2.1 Test specimens

4-point bending tests were performed for three in situ RPC sound barrier panels and three prefabricated RPC sound barrier panels. The detailed diagrams of in situ and prefabricated panels are shown respectively in Fig. 1 and 2. The test method is to apply a load to the front plate. The main parameters of each panel are shown in Table 1.
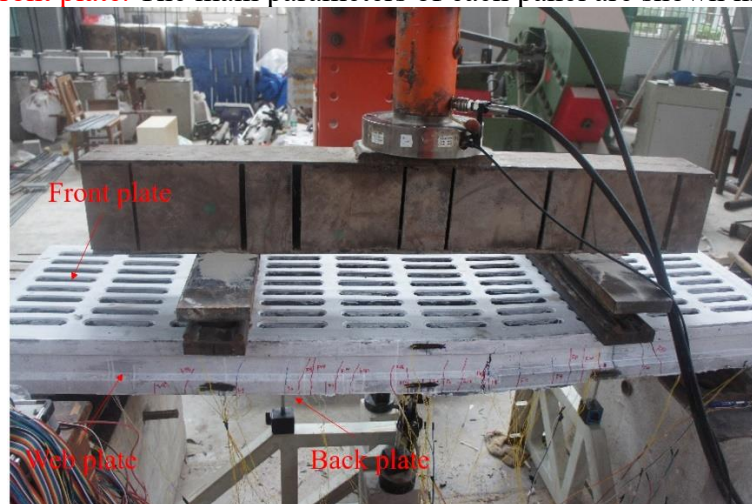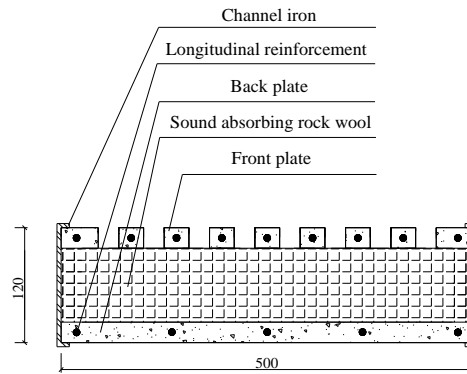

(a) The loading diagram of in situ panels
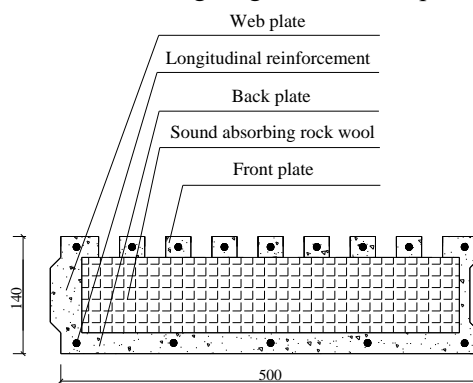
(b) Schematic section diagram of the in situ panel

Figure 1 The detailed diagrams of in situ unit panels

(a) The loading diagram of prefabricated unit panels

(b) Schematic Section diagram of the prefabricated panels

Figure 2 The detailed diagrams of prefabricated unit panels

	Span (mm)	Width (mm)	Overall thickness (mm)	Thickness of front panel(mm)	Thickness of back panel(mm)	Whether to apply prestress	Type of specimens
B1				25	25	No	In situ unit panels
B2			140	25	25	Yes	
B3	1960	500		25	25	Yes	
B4				30	25	Yes	Prefabricated unit panels
B5			120	30	25	No	
B6				20	20	No	

Table 1 The key parameter of each unit panel

2.2 Test material

In this test, the RPC concrete mix ratio for cement, fine sand, medium sand, coarse sand, silica fume, water reducer and water is 1:0.2:0.8:0.2:0.3:0.02:0.23, steel fiber is used with dosage of 2%, the preparation procedure of RPC is as follows. In accordance to test method in the reference [13]，[14] and [15], the mechanical properties of RPC are shown in Table 2.
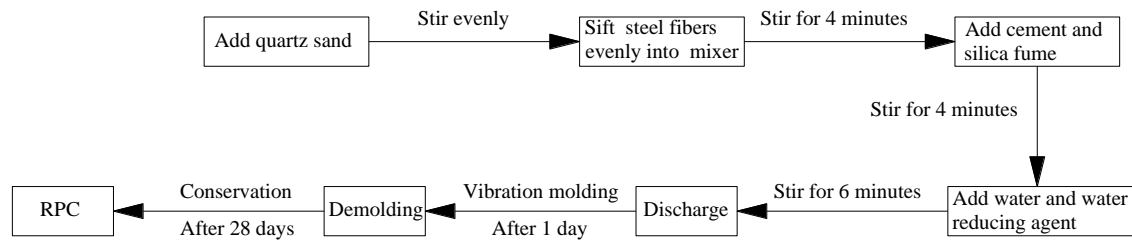
Figure The preparation procedure of RPC

Cube compressive strength f_{cu}(MPa)	Axial compressive strength f_c(MPa)	Splitting tensile strength f_{ts}(MPa)	Axial tensile strength f_t(MPa)
142.6	123.6	7.1	5.3

Table 2 The test value of mechanical properties of RPC

NB：Reference [16], $f_t = 0.75 f_{ts}$.

The yield strength and ultimate strength of steel bars are shown in Table 3.

	Diameter(mm)	Yield Strength (MPa)	Ultimate Strength (MPa)
HRB400	6	466	560

Table 3 The test value of mechanical properties of steel bars

2.3 Prestressing the panels

As it shown in Figure 3, the two ends of the HRB400 steel bars with a diameter of 6mm are processed into threads, which are passed through a pre-made steel plate with holes, and the steel bar is tensioned by tightening the nut. The pre-tension method is used to apply the prestressing force, and the steel bar is stretched at one end. The strain of the steel bar is measured by the DHDAS dynamic signal acquisition and analysis system. From the reinforcement tensioning to the completion of the unit board maintenance, the collection of the reinforcement strain data has been maintained to determine the tensile control stress and effective prestressing of each reinforcement. The manufacturing process of the prestressed unit plate is: laying a rubber plate with convex teeth → supporting form → tensioning panel steel reinforcement → pouring panel concrete → placing sound-absorbing rock wool → tensioning backing plate steel reinforcement → pouring backing plate concrete → curing → releasing prestressed reinforcement.
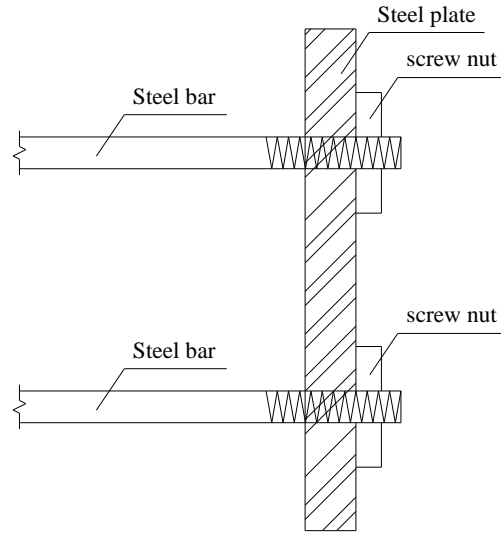
Figure 3 The schematic diagram of steel bar tension

The prestress degree λ represents the degree of prestress applied to the prestressed concrete member. The prestress degree λ is defined as the ratio of the depressurizing bending moment M_0 determined by the magnitude of the prestressing force to the bending moment M generated by the external load. It can also be expressed as the ratio of the prestressed concrete edge compressive stress σ_{pc} generated by the effective prestress to the edge tensile stress σ_{sc} generated under the short-term effect of external load. The degree of prestressing is calculated using formula (1a) and (1b).

$$\lambda = M_0 / M \tag{1a}$$

$$\lambda = \sigma_{pc} / \sigma_{sc} \tag{1b}$$

The prestressed flexural capacity can be calculated by formula (2).

$$M_0 = \sigma_{pc} \cdot W_0 \tag{2}$$

Where, σ_{pc} is the prestressed stress at the tension fiber of the panel ；W_0 is the equivalent elastic moment capacity.

The calculation results of prestressing degree of prestressed panels are shown in Table 4.

	σ_{pc}(MPa)	M_0(kN·m）	M(kN·m）	λ
B2	1.92	2.40	16.45	0.146
B3	2.40	3.00	16.47	0.182
B4	1.22	1.52	10.60	0.143

Table 4 The prestressing degree of prestressed unit panels

3. Experimental results and analysis

3.1 Cracking load and ultimate load

The cracking load and ultimate load of each unit panel are shown in Table 5.

	Overall thickness (mm)	Thickness of front panel(mm)	Thickness of back panel(mm)	λ	Cracking load（kN）			Ultimate load （kN）
					Back panel	Front panel	Web panel	
B1	140	25	25	0	28.1	26.6	32.1	77.0

|								
B2		25	25	0.146	32.1	—	37.5	73.1
B3		25	25	0.182	43.4	39.0	43.4	73.2
B4		30	25	0.143	23.0	19.1	—	35.3
B5	120	30	25	0	21.1	16.7	—	37.4
B6		20	20	0	19.1	14.6	—	26.5

Table 5 The cracking loads and ultimate loads of unit panels

In can be seen from Table 5 that, for the in situ unit panels, when the prestressing degrees increases from 0 to 0.146 and 0.182, the cracking loads of back plates are increased by 14.2% and 54.5%, and the cracking loads of web plates are increased by 16.8% and 35.2%, indicating that the prestressing can effectively increase the cracking loads of the panel units. For the prefabricated panels, the cracking load of back plate of B4 is increased by 9.0% compared with B5, and the cracking load of front plate of B4 is increased by 14.4% compared with B5, indicating that prestressing can increase the cracking load on the unit panel. The cracking load of back plate of B5 is increased by 10.5% compared with B6, and the cracking load of front plate of B5 is increased by 14.4% compared with B6, indicating that increasing the thickness of the back and front plate can increase the cracking load on the panels.

For the in situ panels, the ultimate loads of the three panels are almost the same, indicating that increasing the prestressing degree cannot increase the ultimate bearing capacity of the panels. For the prefabricated unit panels, the ultimate bearing capacity of B5 is not much different from that of B4, indicating that the application of prestress does not improve the ultimate bearing capacity of the panel. The ultimate load of B5 is increased by 41.1% compared with B6, indicating that the ultimate load of the panel is greatly increased by increasing the thickness of the panel.
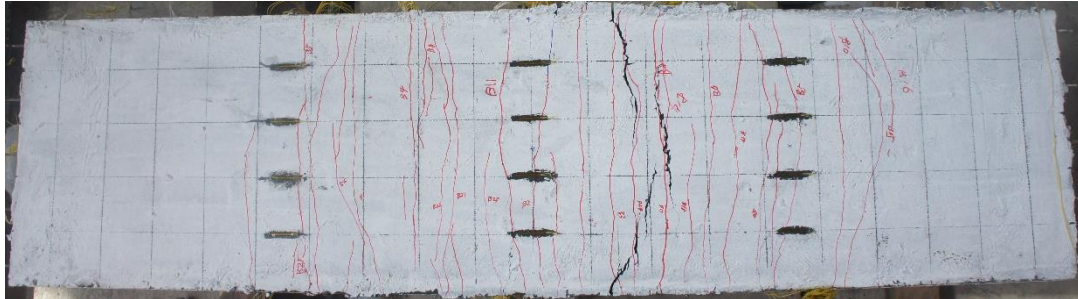
3.2 Failure modes

As it shown in Figure 4, for the in situ unit panels, the failure modes of the non-prestressed panel and the prestressed panels are basically the same. The main cracks are located in the pure bending zone, the cracks in web panels are vertical upwards, and most of cracks of the web panels are connected to the cracks of the back panels, and only a small part of the cracks appear in the curved shear section. The height of the cracks in the web of the panels is the highest in test B1 and B3 is the lowest, indicating that the prestress force can effectively control development of concrete cracks. It can be concluded that, the greater the prestressing degree, the better the effect of limiting crack development.
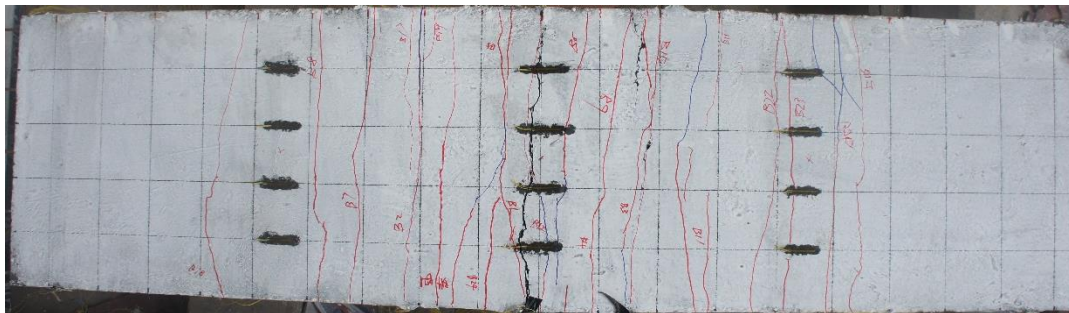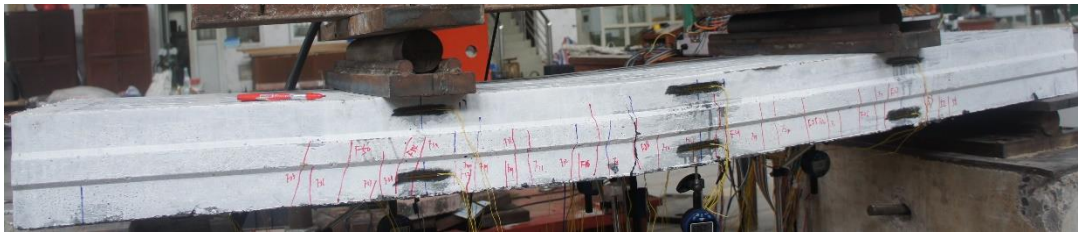

(a) Back plateof B1

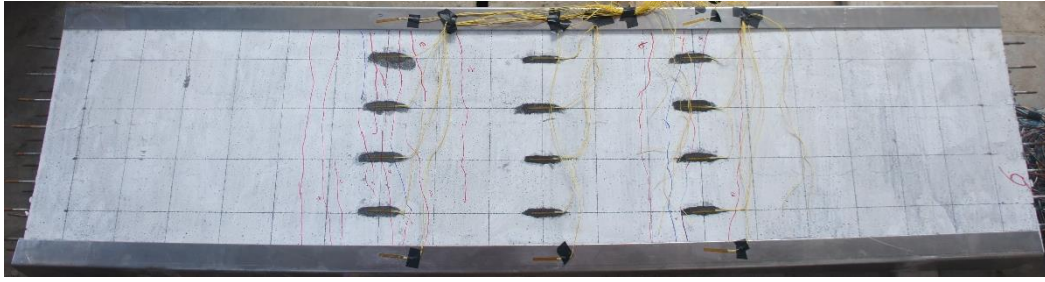(b) Web plate of B1

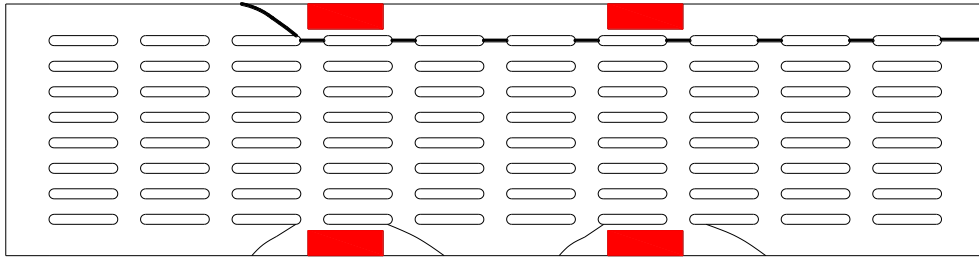(c) Back plate of B2

(d) Web plate of B2

(e) Back plate of B3

(f) Web plate of B3

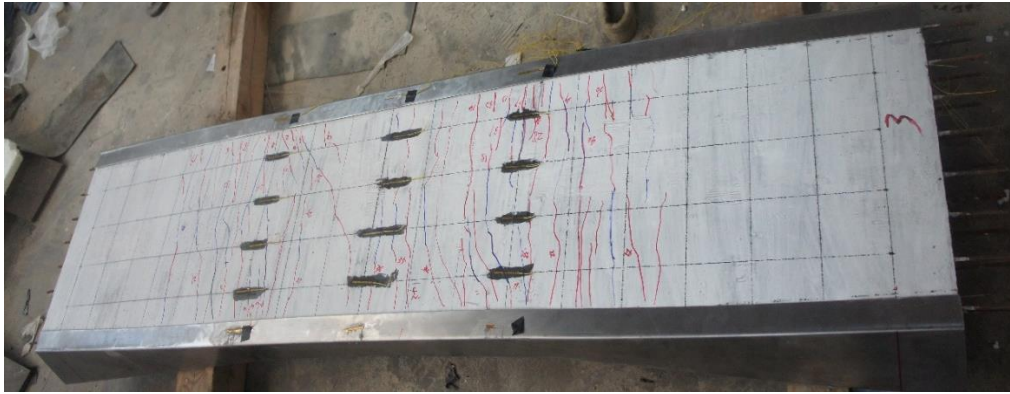**Figure 4 Crack development and failure characteristics of the in situ unit panels**

For the prefabricated panels, the failure modes of the prestressed panel and the non-prestressed panels are basically the same, which are partial damage of the front plates. The reason is mainly that the rigidity of the channel embedment at the front plates is large, which reduces the deflection of the panel. As it shown in Figure 5, The area of the front plate marked in red is the contact area between the front plate and the channel embedments, the thick black lines indicate the cracks in Fig. 5.
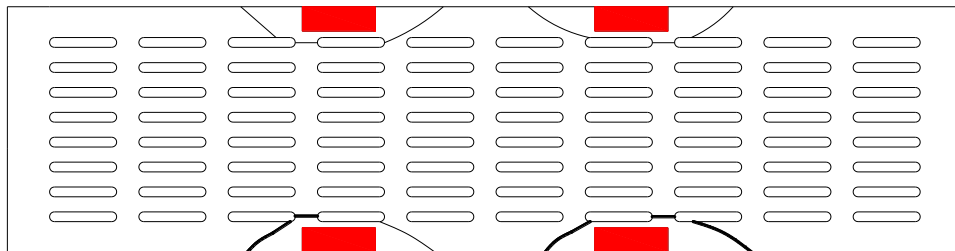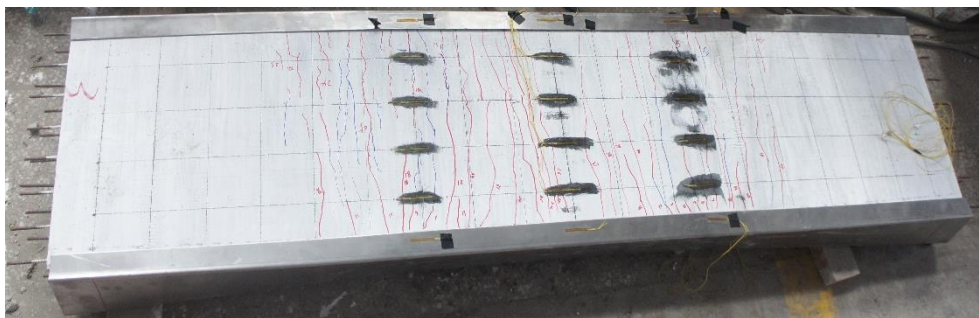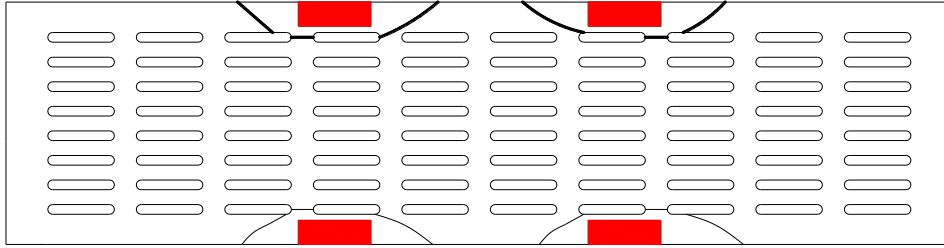
(a) Back plate of B4

(b) Front plate of B4

(c) Back plateof B5
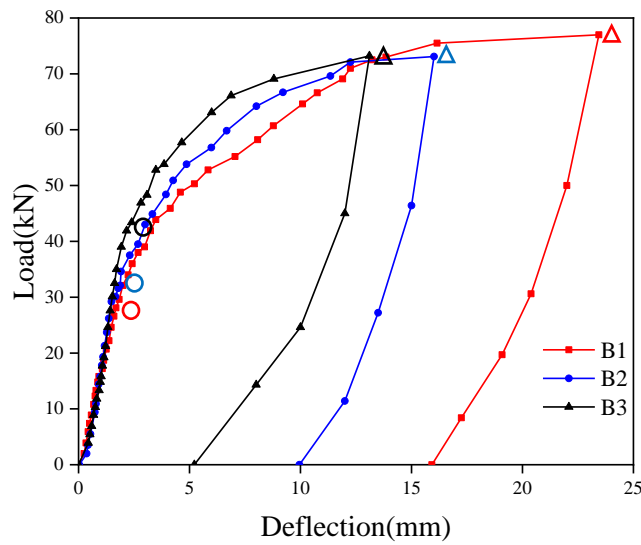

(d) Front plate of B5

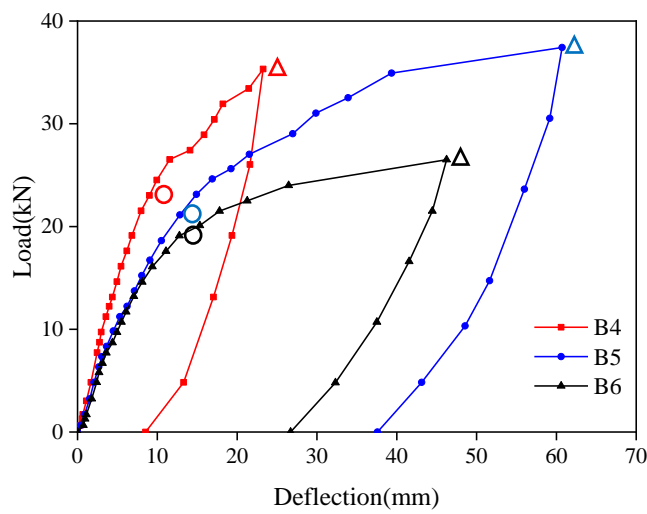

(e) Back plateof B6

（f）Front plate of B6

Figure 5 Crack development and failure characteristics of the prefabricated unit panels

3.3 Deflection of the panels

NB: O indicates the cracking load F_{cr}, Δ indicates the ultimate load F_u.

Figure 6 The mid-span load-deflection curve of the in situ unit panels

NB: O indicates the cracking load F_{cr}, Δ indicates the ultimate load F_u.

Figure 7 The mid-span load-deflection curve of the prefabricated unit panels

It can be seen from Fig. 6 that in the elastic phase, the relationship between the elastic flexural capacity in situ panels is B3>B2>B1, indicating that the increase of the prestressing degree can increase the cracking load of the unit panel. The slope of the load-deflection curve of the in situ panels in the elastic stage is B3>B2>B1, that is, the stiffness of B3 is the largest, the stiffness of B1 is the smallest, indicating that the increase of the prestressing degree can increase the stiffness of the panel.

It can be seen from Fig. 7 that in the elastic phase, the elastic flexural capacity of the prefabricated panels is B4>B5>B6, indicating that the prestressing can significantly increase the cracking load, and increasing the thickness of the back plate and front plate can also slightly increase the cracking load. The slope of the load-deflection curve of the prefabricated panels is B4>B5>B6, indicating that the prestressing can significantly increase the stiffness, and increasing the thickness of the back plate and front plate can also slightly increase the stiffness.

It can be seen from Fig. 6 and Fig. 7 that the deflection of the in situ panel is smaller than that of the prefabricated panel, because the in situ panel has larger flexural rigidity. The residual deformation of the in situ panel is obviously smaller than the prefabricated panel due to the channel embedments in the prefabricated unit panel.

3.4 Ductility of the panels

3.4.1   The coefficient of deflection ductility [17]

The coefficient of ductility can be calculated according to formula (3).

$$\mu_\Delta = \frac{\Delta_u}{\Delta_y} \tag{3}$$

Where，μ_Δ is ductility coefficient, Δ_u is the ultimate deflection；Δ_y is the deflection at yield.
The coefficient of ductility reflects the change of the mid-span displacement of the simply supported beam in the two stages which are the yield state and the ultimate state. The larger the value of the coefficient of ductility, the better the ductility of the . panel.
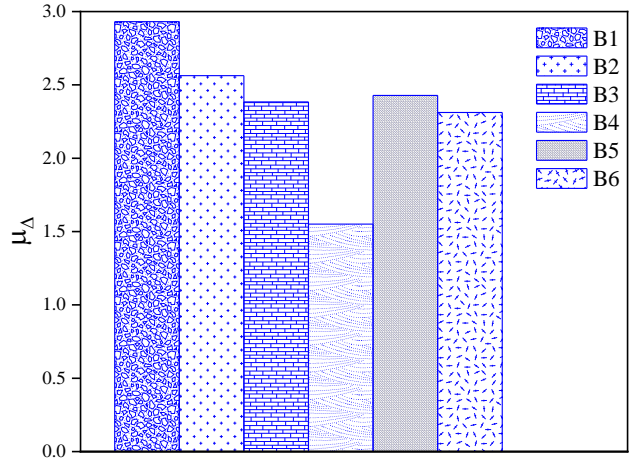
Figure 8 The coefficients of deflection ductility of the unit panels

It can be seen from Fig. 8 that for the in situ unit panels, the relationship of the coefficients of ductility is B1>B2>B3, and the coefficients of ductility of B2 and B3 are reduced by 12.6% and 18.7%, indicating that increasing the degree of prestress will reduce the ductility of the unit panel. The reason is that the application of the pre-stress increases the rigidity of the panel, the development of the deflection of the panel is limited, thereby the ductility of the unit panel is reduced. For the prefabricated panel, the coefficient of deflection ductility of B4 is reduced by 36.1% compared with B5, indicating that the application of prestress obviously reduces the ductility of the panel. The coefficient of ductility of B6 is reduced by 4.8% compared with B5, indicating that reducing the thickness of the back plate and front plate slightly reduces the ductility of the panel

3.4.2   *The energy dissipation factor* [18]

The energy dissipation factor can be calculated according to formula (4).

$$\mu_{in} = \frac{W_{tot} - E_{el}}{W_{tot}} = \frac{U_{in}}{W_{tot}} \qquad (4)$$

Where, W_{tot} is the total energy, E_{el} is the elastic energy, U_{in} is dissipated energy

The energy dissipation factor is also one of the criteria for evaluating the ductility of the member. The energy dissipation factor of the member is obtained by calculating the energy consumption of the members.
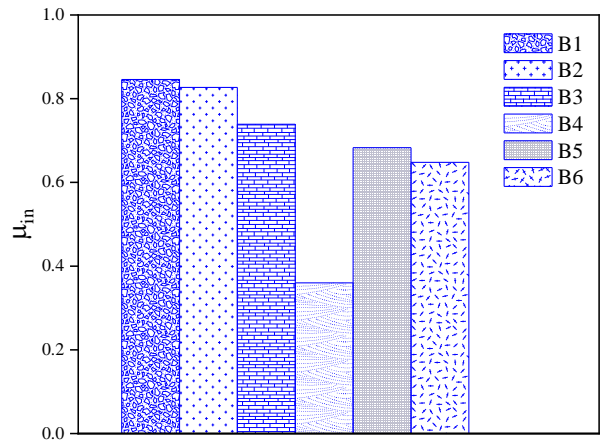
Figure 9 The energy dissipation factors of the unit panel

It can be seen from Fig. 9 that for the in situ unit panels, the relationship of the energy dissipation factors is B1>B2>B3, and the energy dissipation factors of B2 and B3 are reduced by 2.2% and 12.6% compared with B1, indicating that the increase of prestressing degree will reduce the ductility of the unit panel. For the prefabricated unit panels, the energy dissipation factor of B4 is reduced by 47.3% compared with B5, indicating that prestressing will obviously reduce the ductility of the unit panel. And the energy dissipation factor of B6 is reduced by 5.1% compared with B5, indicating that reducing the thickness of the back and front plate will slightly reduce the ductility of the unit panel. In addition, after the pre-stress is applied, the energy dissipation factor of the prefabricated unit panel is reduced to a greater extent than that of the in situ panel. It is due to the enhanced rigidity of the channel embedments of the prefabricated panel, the overall energy dissipation capability is not as good as that of the in situ unit panel. The energy dissipation of the prefabricated unit panel is suddenly reduced after the application of prestressing, and the ductility loss is very obvious.

4. Formula to Calculate the flexural capacity of the in situ panels

4.1 Simplified section of the in situ panels

The in situ panel consists a back plate, a front plate and a web plate, the cross-section of the panel can be simplified into an I-shaped section as shown in Fig. 10[19].
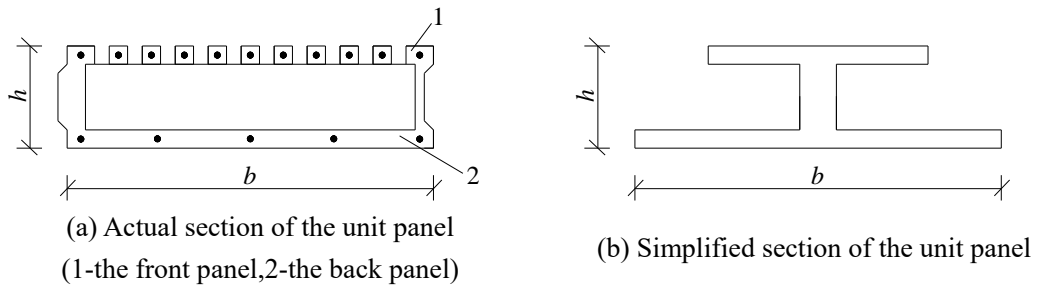

(a) Actual section of the unit panel
(1-the front panel,2-the back panel)

(b) Simplified section of the unit panel

Figure 10 Simplified diagram of section of the unit panel

4.2 Moment at crack for in situ unit panels

Under the bending load, the cracking loads of the panels are mainly determined by the tensile strength of RPC and the pre-stressing value. The cracking moment of the panels can be calculated according to formula (5).

$$M_{cr} = (\gamma f_t + \sigma_{pc})W_0$$

（5）

Where, M_{cr}^c is the cracking movement ,γ is the safety factor , taken as 1.35 according to Chinese design code [22]

Table 6 shows the comparison of M_{cr}^c based on formula (5) and the actual cracking moment M_{cr}^t from the tests.

λ	the calculated value M_{cr}^c / kN·m	the experimental value M_{cr}^t / kN·m	M_{cr}^c / M_{cr}^t

B1	0	8.15	8.43	0.9663
B2	0.146	10.61	9.63	1.1026
B3	0.182	11.52	13.02	0.8841
		Average value		0.9844
		Standard deviation		0.0901
		Coefficient of variation		0.0916

Table 6 The comparison between the calculated and experimental values of the cracking moment of the panels

It can be seen from Table 6 that the calculated and experimental values of the cracking moment of the panels increase with the increase of the prestressing degree, and the calculated values is in good agreement with the experimental values. Therefore, formula (5) can be used as a calculation formula for the cracking moment of the in situ prestressed RPC sound barrier panels.

4.3 Flexural capacity of the in situ panels

Unlike the ordinary concrete, the tensile strength of reactive powder concrete is higher. After the member is cracked, the concrete at the crack can still bear a certain tensile stress due to the presence of steel fiber. Therefore, it cannot be ignored when calculating the flexural capacity. As it shown in Figure 11, by calculating the section type of the panels, it is concluded that the section type of the panels belongs to the second type of I-shaped section.
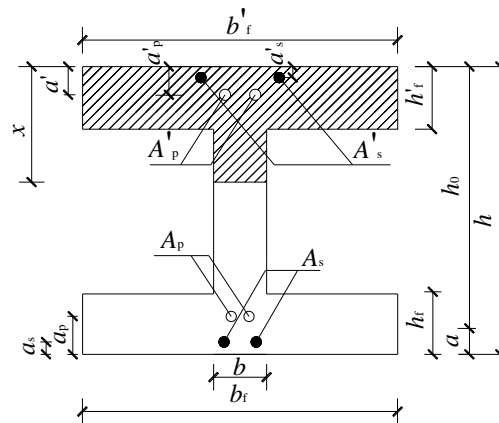

Figure 11 Schematic diagram of the height of compression zone of the I-shaped section

Considering the boundary damage, the prestressed steel bars of the tension zone reach the design value, and the concrete on the compression edge of the section is crushed. In the case of failure, the prestressed steel bars placed in the compression zone do not reach yield strength regardless of tension or compression, and approximately $\sigma'_p=\sigma'_{p0}-f'_{py}$ is used to simplify the calculation.

(a) Actual stress distribution map   (b) equivalent stress distribution map
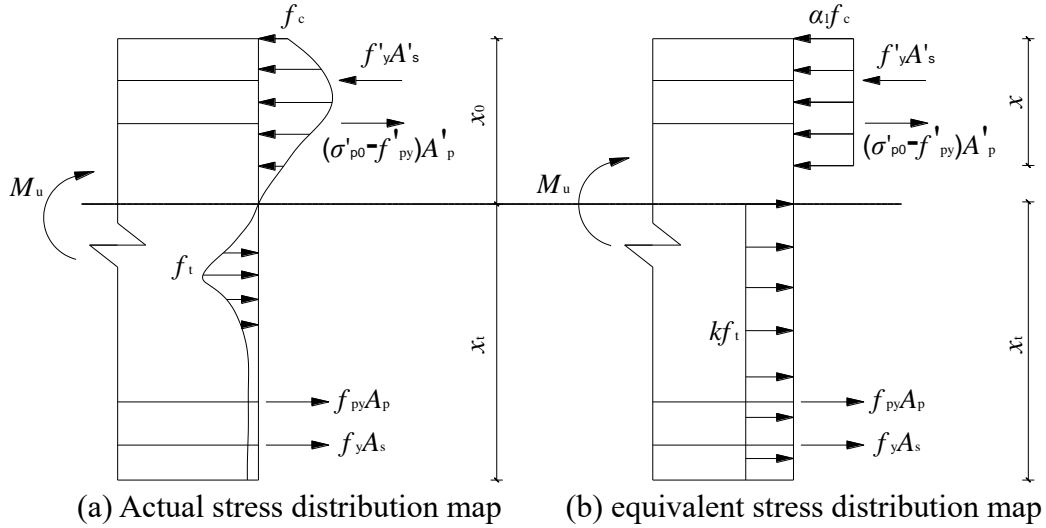
Figure 12 Section stress block

According to the stress block shown in Figure 12, the flexural capacity is calculated using:

$$M \le M_u = \alpha_1 f_c b \ (h_0 - x/2) + \alpha_1 f_c (b_f' - b) h_f (h_0 - h_f'/2) + f_y' A_s' (h_0 - a_s')$$
$$- (\sigma_{p0}' - f_{py}') \ A_p' (h_0 - a_p') - k f_t b x_t (x_t/2 - a) - k f_t (b_f - b) h_f (h_f/2 - a) \quad (6)$$

and:

$$\alpha_1 f_c b x + \alpha_1 f_c (b_f' - b) \ h_f' = f_y A_s - f_y' A_s' + f_{py} A_p + (\sigma_{p0}' - f_{py}') \ A_p'$$
$$+ k f_t b x_t + k f_t (b_f - b) \ h_f \quad (7)$$

The calculated value of the ultimate capacity is compared with the experimental value. The results are shown in Table 7.

	the calculated value M_u^c/kN·m	the experimental value M_u^t/kN·m	M_u^c / M_u^t
B1	18.30	17.33	1.0562
B2	16.69	16.45	1.0133
B3	18.29	16.47	1.1106
	Average value		1.0600
	Standard deviation		0.0398
	Coefficient of variation		0.0376

Table 7 The comparison between the calculated and experimental values of the ultimate bending moment of the unit panels

It can be seen from Table 7, the calculated values are larger than the experimental values, which is due to the special structural form of the sound barrier unit panels, but the difference is not large

4.4 Calculations of crack width and deflection for in situ panels

4.4.1   Calculation of maximum crack width

With reference [15] to the concrete structure design specification, the maximum crack

width is calculated according to formula (8).

$$\omega_{\max} = \alpha_{cr} \cdot \psi \frac{\sigma_{sk}}{E_s} l_c = \alpha_{cr} \cdot \psi \frac{\sigma_{sk}}{E_s} \cdot c_f (1.9c + 0.08 \frac{d_{eq}}{\rho_{te}})$$

（8）

The nature of the crack width of the flexural member is the relative strain difference between the steel bar and the concrete. The incorporation of steel fiber is an effective measure to control the cracking of concrete. The crack width of the unit panel is related to the volume ratio, the aspect ratio and the bonding property of the steel fiber. Therefore, the formula (8) needs to be modified. The effect of steel fiber on the maximum crack width is now discussed.

4.4.1.1 The coefficient of force characteristics αcr

The coefficient of force characteristics includes the influence of four parameters, which can be modified according to formula (9).

$$\alpha_{cr} = \tau_1 \tau_2 \tau_3 \alpha_c$$

（9）

τ_1 is the coefficient of long-term effect, according to the Chinese concrete structure design specification, τ_1 takes 1.5, τ_2 is the ratio of maximum crack width to average crack width, reference [20], τ_2 takes 1.6,τ_3 is the coefficient of working conditions of the concrete member，for bending member, τ_3 takes 1.0,α_c is the influence coefficient of average strain of concrete in the tension zone，according to the Chinese concrete structure design specification, α_c approximately takes 0.77.

4.4.1.2 Stress of tensile reinforcement

Due to the high strength of RPC and the incorporation of steel fiber, the stress of the rebar in the panel will decrease with the increase of the strength of the matrix and the increase of the dosage of the steel fiber. The formula (8) has been modified to the formula (10) in the reference [21].
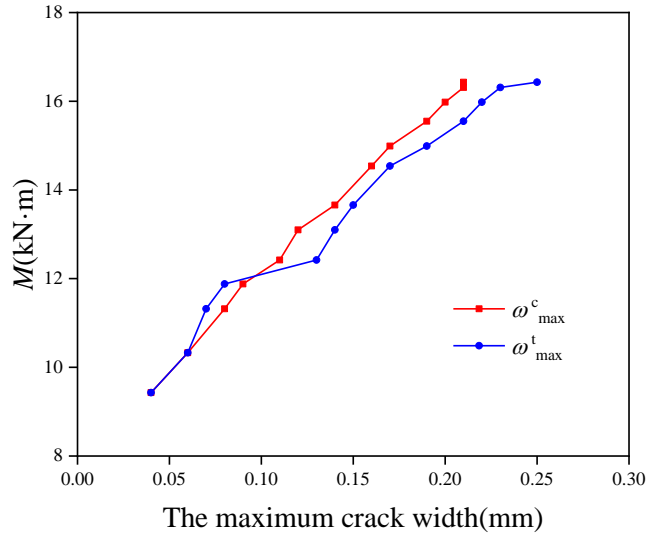
$$\omega'_{\max} = \omega_{\max}(1 - \beta_{cw} \frac{f_t \lambda_f}{\rho_s \sigma_{sk}})$$

（10）

β_{cw} is mainly related to the type of steel fiber, reference [22], for shearing straight fibers, β_{cw} takes 0.35.
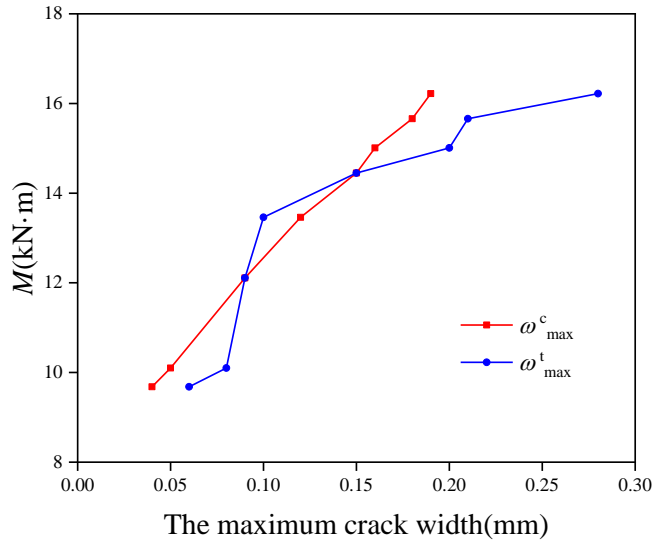
In summary, formula (11) is the modified formula for calculating the maximum crack width of the unit panel.

$$\omega_{\max} = \alpha_{cr} \psi \frac{\sigma_{sk}}{E_s} (1.9c + 0.08 \frac{d_{eq}}{\rho_{te}}) \quad (1 - \beta_{cw} \frac{f_t \lambda_f}{\rho_s \sigma_{sk}})$$
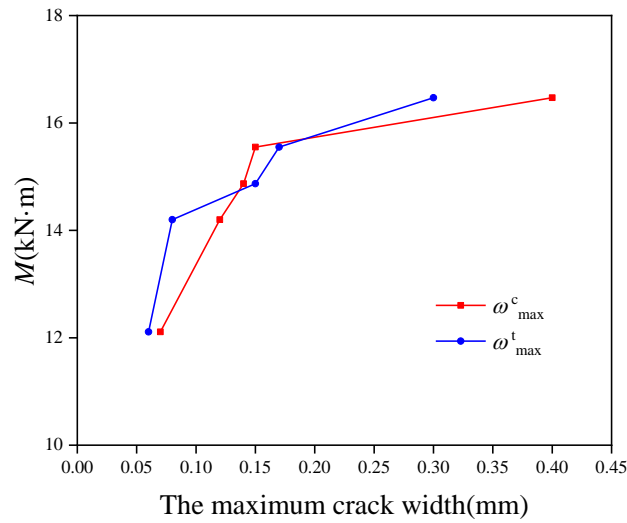
（11）

As shown in Fig. 13, the calculated values of maximum crack width are compared with the experimental values.

(a) B1

(b) B2

(c) B3

Figure 13 Contrast curves between calculated values and experimental values of maximum crack width of the unit panels

It can be seen from Fig. 13 that when the flexural capacity is in the range of 0.6 M_u

to 0.95 M_u, the formula (11) can relatively accurately calculate the maximum crack width under each load. After the crack occurs in the panel, the crack propagation is in a relatively stable stage due to the bonding of the steel fiber at the crack. At this stage, the maximum crack width value of the panel can be calculated accurately. When the steel bar reaches the yield strength, the crack develops rapidly, the crack width increases significantly, and the steel fiber at the crack is continuously pulled out or broken, resulting that the inaccuracy of formula (11).

4.4.2 Calculation of deflection

Since the prestressing stress applied to the concrete by the prestressing bars in the back plate and the front plate are substantially the same, the prestressed concrete flexural members that allow cracks to occur, the short-term stiffness B_s can be calculated according to formula (12)[15].

$$B_s = \frac{0.85E_cI_0}{\kappa_{cr} + (1-\kappa_{cr}) \ \omega}$$

（12）

The aspect ratio, shape and type of steel fiber will affect the stiffness of the bending members after cracking. Under the normal circumstance, steel fiber can increase the stiffness of the members by 10%~40% after cracking. Considering the test results, the reference [23] uses data regression for simplified calculations.

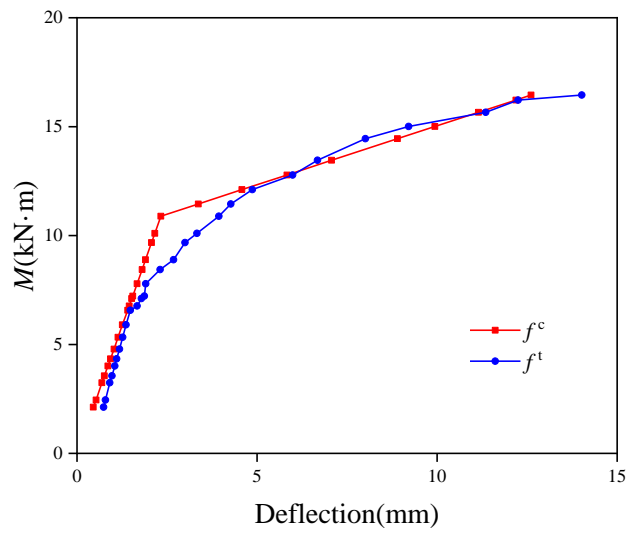$$B_s^c = B_s(1+\beta_B\lambda_f)$$

（13）

According to the calculation method of the deflection deformation of the simply supported bending members in the material mechanics, the deflection of the unit panel is calculated by the formula (14).

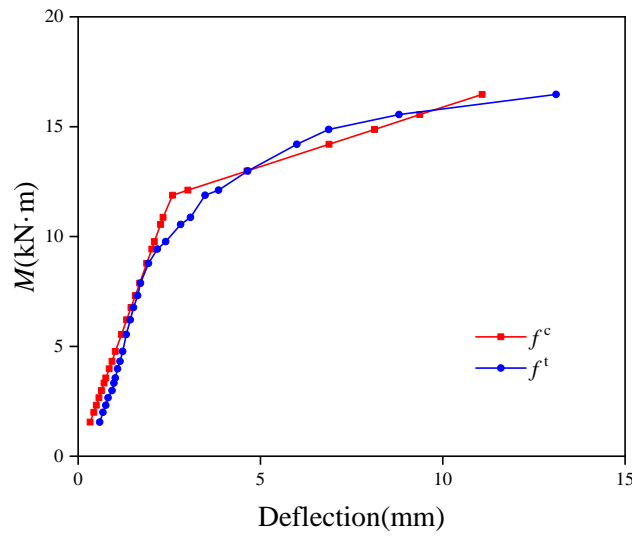$$f = \frac{11Pl^3}{384B_s}$$

（14）

As shown in Fig. 14, the calculated values of deflection are compared with the experimental values.
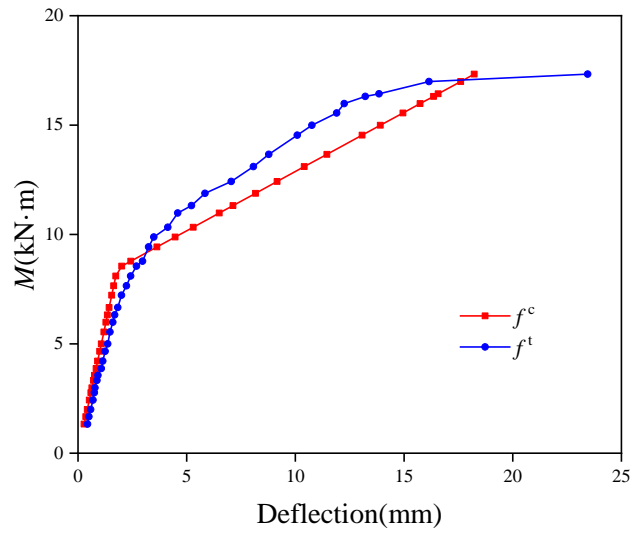
(a) B1

(b) B2

(c) B3

Figure 14 Comparison between calculated values and experimental values of deflection deformation of the unit panels

It can be seen from Fig. 14 that the calculated deflection curve of the panels tends

to be consistent with the deflection curve from the tests. Before cracking, the stiffness of the unit panel changes little, so the calculated deflection curve agrees well with the experimental results. After cracking, compared with B2 and B3, the calculated deflection curve of B1 has a larger error. The reason is that B2 and B3 are prestressed panels, the crack widths are smaller than B1, and the stiffness changes are more stable than B1. Therefore, their calculated values of the deflection are in good agreement with the experimental values.

5. Conclusion

1. Prestressing can effectively improve the cracking loads of the in situ and prefabricated unit panels, but it cannot increase the ultimate flexural capacity of the unit panels. For the prefabricated panels, increasing the thickness of the back and front plate can increase the cracking load and ultimate load.

2. For the in situ panels, the bending failure occurs in each unit panel. Increasing the prestressing degree can increase the rigidity of the unit panel, but it will reduce the ductility of the unit panel. For the prefabricated unit panels, due to the rigidity enhancement of the channel embedments, the flexural deflection of the panel is smaller, resulting in partial damage of the front plate of each unit panel. Prestressing or increasing the thickness of the back and front plate can increase the rigidity of the unit panel, but it will reduce the ductility of the unit panel.

3. By modifying the existing calculation method of the conventional prestressed concrete flexural members, the calculation formula for the panels is obtained. The calculated values of the cracking moment are in good agreement with the experimental values, and the calculated values of ultimate bending moment are larger than the experimental values due to the special structural form of the unit panels.

4. Based on the test results, considering the "bridge" effect of steel fiber, the formula to calculate the crack width and deflection in service limit stage are developed. The calculated values of the prestressed panels are in good agreement with the experimental values.

Reference

[1] Huang Cheng-kui. Fiber Concrete Structure. Beijing, Mechanical Industry Press, 2004.
[2] Cao Xia, Chang Jing, Wang Yan-jun. Experimental study on bearing capacity of normal section of flexural members of high strength steel RPC beams. Journal of Henan University of Technology (Natural Science),2015,34(01), pp109-115.
[3] Wu Xin-ke. Experimental study on the crack resistance of normal section of RPC beam with high strength steel. Guilin University of Technology,2014.
[4] Yan Xin. Preparation technology and curing method of reactive powder concrete.

China Building Materials Science and Technology, 2017, 26 (2), 32

[5] Yang Zhi-hui. Study on tensile mechanical properties of reactive steel reinforced concrete with different steel fibers. PhD Thesis. Beijing Jiao tong University, 2006.

[6] Wang Qiang. Research on shear resistance of HRB500 grade steel reactive powder concrete beam, PhD Thesis, Guangxi University, 2017.

[7] Xu Hai-bin, Deng Zong-cai, Chen Chun-sheng, Chen Xing-wei. Experimental study on shear behavior of ultra-high performance fiber concrete beams[J].China Civil Engineering Journal,2014,47(12):91-97.

[8] Homma S, Susuki T,Hanada N,et al.Wind response of constitutive members of a tower-supported steel stack, Proceeding of 18th National Symposium on Wind Engineering.2004:479-484.

[9] G.R. Watts, P.A. Morgan, M. Surgand. Assessment of the diffraction efficiency of novel barrier profiles using an MLS-based approach, Journal of Sound and Vibration, 2004(274): 669-683.

[10] Zhang Ji-wen, Zeng Jun-cheng, Zhang Zhen-xing, Tu Yong-ming, Lü Jian-pin. Experimental study on bending-compression fatigue behavior of prestressed concrete, Industrial Construction,2009,39(08):72-75.

[11] Lü Jian-pin, Zhang Ji-wen, Liao Jian-zhou, Hu Wei-nan, Tu Yong-ming. Pulsation-induced wind-induced response of high-speed trains with existing railway bridges, Journal of Southwest Jiao tong University,2009,44(04):547-551.

[12] He Li-ping. Theoretical analysis and experimental study on the flexural capacity of the positive section of the GRC high-speed railway acoustic barrier. PhD Thesis. Beijing Jiaotong University, 2013.

[13] National Standard GB/T 31387—2015 Reactive Powder Concrete, Beijing: China Building Industry Press, 2015.

[14] National Standard GB/T 50152—2012 Standard for test method of concrete structures, Beijing: China Building Industry Press, 2012.

[15] National Standard GB50010-2010 Code for Design of Concrete Structures，Beijing: China Building Industry Press, 2015.

[16] Graybeal B A. Characterization of the behavior of Ultra-High-performance concrete, PhD Thesis. American: The University of Maryland, 2005.

[17] Zhou Zhi-xiang. Higher reinforced concrete structure, Master Thesis. Beijing: China Communications Press, 2002.

[18] Meng Lü-xiang. Study on the bending behavior of partially prestressed concrete beams with fiber reinforced plastics, PhD Thesis. China Academy of Building Research, 2005.

[19] Huang Jia-zhu. Application research of high-speed railway plug-in concrete sound barrier unit board in typhoon area, PhD Thesis Guilin University of Technology, 2016.

[20] Li Li. Study on the mechanical properties and design method of reactive powder concrete beam, PhD Thesis. Harbin Institute of Technology, 2010.

[21] Finite Element Analysis of Concrete Structures [M]. Beijing: Tsinghua University Press, 2005.

[22] Huang Cheng-kui, Zhao Guo-fan, Wang Zhi-jie. Calculation method of crack width of steel fiber reinforced concrete flexural members. Journal of Dalian University of Technology, 1993, 33(5): 558-565.

[23] Zhao Guo-fan, Peng Shao-min, Huang Cheng-kui. Steel fiber concrete structure PhD Thesis. Beijing: China Building Industry Press, 1999.